ChemComm

COMMUNICATION

View Article Online
View Journal | View Issue

Cite this: *Chem. Commun.*, 2021, **57**, 2305

Received 16th December 2020,
Accepted 21st January 2021

DOI: 10.1039/d0cc08162k

rsc.li/chemcomm

A two-pronged photodynamic nanodrug to prevent metastasis of basal-like breast cancer†

Jing Zhang, Ningning Wang, Qian Li, Yaxin Zhou and Yuxia Luan *

A two-pronged concept combining photodynamic therapy (PDT) and epithelial–mesenchymal transition (EMT) blockade in a minimalist nanoplatform was proposed to combat basal-like breast cancer (BLBC) metastasis. Based on PDT-mediated tumor killing and epalrestat (Epa)-mediated EMT blockade, as-prepared Ce6/Epa nanoparticles prevented BLBC metastasis effectively *in vivo*, providing a very promising two-pronged strategy against BLBC metastasis.

Basal-like breast cancer (BLBC) is the most aggressive subtype of breast cancer, characterized by a high grade, poor prognosis and distant metastasis.[1] Due to its insensitivity to hormone therapy and targeted therapy, the clinical outcome for BLBC treatment is unsatisfactory.[2,3] Metastasis accounts for the most death cases due to BLBC.[4] Exploiting a highly efficient strategy to impede distant metastasis from BLBC has become a major challenge.

Studies have shown that chemotherapeutic or phototherapeutic nano delivery systems could reduce metastasis by having enhanced tumor-killing efficiency.[5,6] However, such strategies have overlooked what happens in tumor cells during metastasis, thereby leading to suboptimal results. In general, illumination of the underlying mechanisms of metastasis is important for planning interventions. Metastasis is a complicated and multistep biological event. The tumor undergoes changes initially, especially the promotion of invasiveness to dissemination from the primary tumor. Then, the disseminated tumor cells circulate and "seed" in suitable beds.[7] Therefore, targeting any step of metastasis could be beneficial for treatment.[8,9] In particular, very recent advances in nanodrugs targeting different metastasis steps have offered promising alternatives, such as killing disseminated tumor cells in lymph nodes,[10] modulating the premetastatic *niche* to prevent disseminated tumor cells from seeding in distant organs[11,12] or treating the metastatic tumor.[13] Nevertheless, more attention has been attached to killing metastatic cells instead of preventing their initial dissemination. It would be more practical to prevent metastasis before it begins rather than treating it after it has happened.

Epithelial–mesenchymal transition (EMT) is a complicated process closely associated with the invasiveness of epithelial tumors.[14] Changes in cells undergoing EMT begin with the loss of the epithelial marker E-cadherin (E-cad), which is a constituent of adherent junctions. This action is followed by the acquisition of the pro-migratory mesenchymal marker N-cadherin (N-cad), which results in the dissemination of tumor cells from epithelial sheets and acquisition of invasiveness.[14] EMT is highly activated in BLBC. Therefore, invasiveness acquisition with EMT in BLBC could be a valuable target against metastasis.

Aldo-keto reductase family 1 member B1 (AKR1B1) is overexpressed and plays a key part in facilitating BLBC progression and activating EMT.[15] An inhibitor of AKR1B1 called epalrestat (Epa) has been demonstrated to inhibit tumor progression and extinguish the invasiveness of BLBC.[15] Unfortunately, although Epa can also act as a antitumor agent, its tumor-inhibition capability is weaker than that of widely applied chemotherapy agents or phototherapy. Moreover, the molecular mechanism of action of Epa involves a reduction in the levels of cytotoxic reactive oxygen species (ROS),[15] so tumor cells are not killed. ROS are of particular importance in tumor treatment because they can trigger apoptosis directly or work as substrates in various catalysis reactions.[16] To reverse these disadvantages, photodynamic therapy (PDT) could be introduced because it produces abundant ROS to kill tumor cells, is minimally invasive and has high spatiotemporal specificity. Thus, the drawbacks of using Epa against metastasis (*i.e.*, unsatisfactory tumor-inhibition capability) could be overcome. Therefore, a "two-pronged" approach could combine PDT and Epa to kill tumor cells and block EMT, respectively. Chlorin e6 (Ce6) is the most popular photosensitizer in PDT due to its high singlet oxygen ($^1O_2$) yield,[17] so it was selected as the model photosensitizer in the present study. Epa is strongly hydrophobic, so co-delivery of these two drugs with high drug loading is another

Department of Pharmaceutics, Key Laboratory of Chemical Biology (Ministry of Education), School of Pharmaceutical Sciences, Cheeloo College of Medicine, Shandong University, Jinan, Shandong, 250012, China.
E-mail: yuxialuan@sdu.edu.cn

† Electronic supplementary information (ESI) available: Experimental section and Fig. S1. See DOI: 10.1039/d0cc08162k

challenge to be solved. A minimalist drug-delivery strategy without additional carriers, which is called "co-assembly nanotechnology", could self-deliver multiple drugs.[18] Inspired by this concept, we aimed to construct a Ce6 and Epa co-assembled system. To the best of our knowledge, this is the first of a minimalist strategy combining PDT and EMT blockade to prevent BLBC metastasis.

For the proof of concept, Ce6 was co-assembled with Epa to obtain Ce6/Epa nanoparticles (NPs) driven by π–π interactions with 100% drug loading. When the Ce6/Epa NPs reached a tumor site, they would work from two aspects. First, they would kill tumor cells with enhanced tumor accumulation and ROS generation by nanoscale Ce6-based PDT under near infrared (NIR) laser irradiation. Second, they would reduce invasiveness with Epa-mediated EMT blockade. This two-pronged nanoplatform was demonstrated to help prevent BLBC metastasis *in vitro* and *in vivo*, thereby providing a novel and valuable approach for cancer treatment.

In the present work, Ce6/Epa NPs were fabricated *via* co-assembly nanotechnology in which π–π interactions act as the main driving force. To validate formation of the co-assembled NPs, a sample of free Epa and sample of free Ce6 were also prepared. After stirring, large aggregations were observed in the Ce6 sample and Epa sample (Fig. S1a, ESI†), and most aggregations precipitated by the next day. Surprisingly, the Ce6/Epa NPs were a homogeneous solution which remained stable after 1 month. The absolute difference between the Epa, Ce6 and the Ce6/Epa NPs in terms of physical stability demonstrated the successful assembly of Ce6 with Epa. Furthermore, the shift in the absorbance peak between monomeric Ce6 (Ce6/Epa NPs in a mixed solvent) and co-assembled NPs indicated the π–π stacking in Ce6/Epa NPs (Fig. S1b, ESI†). The mean particle size was measured to be 144.9 nm (Fig. 1a). The inset transmission electron microscopy (TEM) image in Fig. 1a shows that the Ce6/Epa NPs have a uniform and spherical morphology. The zeta potential was recorded as −30.2 mV (Fig. S2, ESI†). This zeta potential of the Ce6/Epa NPs might have contributed to the excellent physical stability of the Ce6/Epa NPs. Moreover, the Ce6/Epa NPs have excellent physiological stability in 10% FBS (Fig. S3, ESI†), suggesting only a slight leakage in the circulation of Epa.

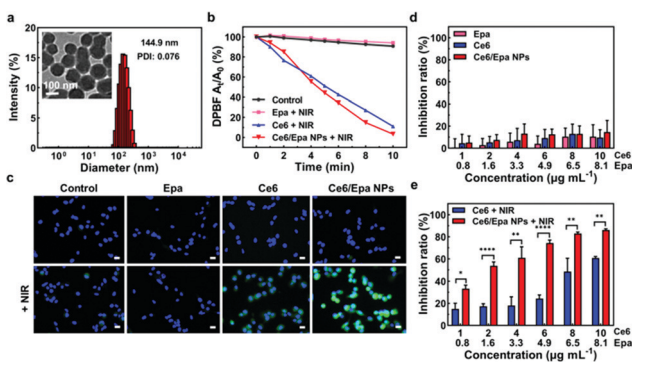

Fig. 1 (a) Particle size and morphology of the Ce6/Epa NPs. (b) $^1O_2$-Generating ability of Epa, Ce6 and the Ce6/Epa NPs under NIR laser irradiation. (c) Fluorescence images showing intracellular ROS generation in differently treated cells with or without NIR laser irradiation. Scale bar = 20 μm. (d) Dark cytotoxicity of Epa, Ce6 and the Ce6/Epa NPs (n = 3) and (e) photodynamic cytotoxicity of Ce6 and the Ce6/Epa NPs (n = 3).

The $^1O_2$-generating ability of the Ce6/Epa NPs under NIR laser irradiation was investigated with a 1,3-diphenylisobenzofuran (DPBF) probe to evaluate the photodynamic capability. The more $^1O_2$ that was produced, the less DPBF that remained. The $^1O_2$-generating ability of Epa after different periods of NIR laser irradiation was negligible (Fig. 1b). Besides this, similar $^1O_2$-generating ability was observed for the Ce6 and Ce6/Epa NPs under NIR laser irradiation. Hence, the NP formation *via* a co-assembling strategy had a negligible influence on the photodynamic capability. In addition, Epa could be released from the Ce6/Epa NPs (Fig. S4, ESI†), which provided a solid foundation for an Epa-mediated EMT blockade.

Flow cytometry was utilized to investigate if the well-designed Ce6/Epa NPs obtained by a co-assembling strategy could be internalized by a human cell line of BLBC cells (MDA-MB-231 cells). The intracellular fluorescence intensity of Ce6 from the Ce6/Epa NP group was much higher than that from the Ce6 group (Fig. S5 (ESI†)), thereby demonstrating NP-enhanced cellular internalization. Fig. 1c and Fig. S6 (ESI†) represent cellular ROS by measurement of green DCF fluorescence *via* a fluorescence microscope and flow cytometer, respectively. There was brighter green fluorescence in the Ce6/Epa NPs-irradiated cells (100 mW cm^{-2}, 2 min) than that in the Ce6-irradiated and un-irradiated cells (Fig. 1c). AKR1B1 is a monomeric enzyme in the cytoplasm that can catalyze the NADPH-dependent reduction reaction. Epa can inhibit AKR1B1, leading to a decrease in cellular ROS generation.[15] The fluorescence intensity in the Ce6/Epa NPs group was slightly weaker than that in the Ce6 group (Fig. S6a, ESI†). However, owing to the excellent ROS generation of Ce6 upon NIR laser irradiation, the ROS decrease caused by Epa was offset in the Ce6/Epa + NIR group compared with that in the control + NIR group (Fig. S6b, ESI†). More importantly, thanks to NP-enhanced cellular internalization, ROS production in the Ce6/Epa NPs + NIR group surpassed that in the Ce6 + NIR group even if Epa in the Ce6/Epa NPs could decrease the cellular concentration of ROS (Fig. S6b, ESI†). To evaluate the photodynamic cytotoxicity of the Ce6/Epa NPs to the MDA-MB-231 cells, the MTT assay was carried out. Ce6 and the Ce6/Epa NPs demonstrated low cytotoxicity without NIR laser irradiation (Fig. 1d), indicating that they had good biocompatibility and low dark cytotoxicity. Although Epa has been reported to have antitumor effects,[19] its efficiency was relatively limited within the concentrations we studied. Surprisingly, when the Ce6- or Ce6/Epa NP-treated cells were irradiated with a NIR laser (100 mW cm^{-2}, 2 min), the Ce6/Epa NPs + NIR were significantly better than Ce6 + NIR in inhibiting tumor cells (Fig. 1e). The strong anti-tumor effects of the Ce6/Epa NPs *in vitro* upon NIR laser irradiation could be attributed to highly efficient internalization (Fig. S5, ESI†). Taken together, these data suggest that the Ce6/Epa NPs are superior in terms of improving internalization and the outcome of photodynamic treatment *in vitro* compared with that using free Ce6.

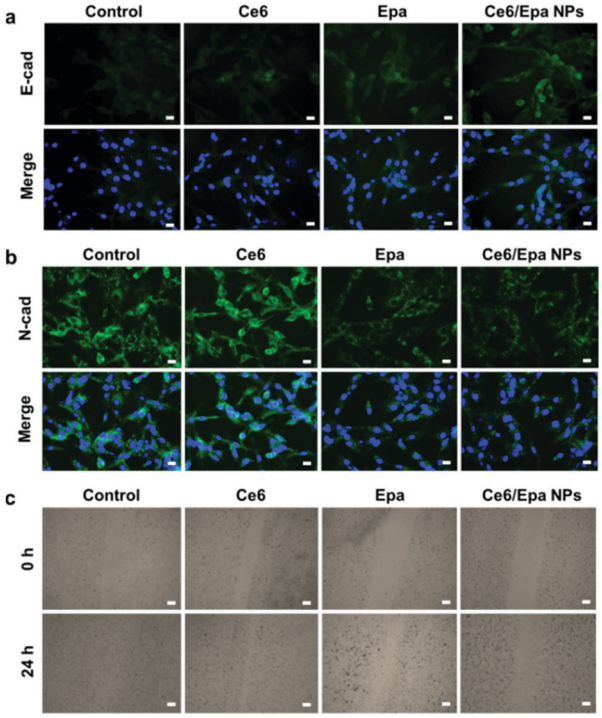

Fig. 2 (a) E-cad expression in differently treated cells. Scale bar = 20 μm. (b) N-cad expression in differently treated cells. Scale bar = 20 μm. (c) Would-healing assay showing the invasiveness of differently treated cells. Scale bar = 200 μm.

Expression of E-cad and N-cad in differently treated MDA-MB-231 cells was analyzed by immunofluorescence staining (Fig. 2a and b, respectively). Expression of E-cad in cells exposed to Epa or the Ce6/Epa NPs was upregulated slightly (Fig. 2a). Epa and the Ce6/Epa NPs reduced expression of the mesenchymal marker N-cad significantly, whereas Ce6 showed no difference, which demonstrated the strong ability of Epa to inhibit EMT (Fig. 2b). To further validate the important role that EMT plays in invasiveness, a wound-healing assay was conducted. The wound in the control or Ce6 groups healed after 24 h of incubation (Fig. 2c), thereby showing the high invasiveness of MDA-MB-231 cells. Importantly, due to the EMT-inhibition effects of Epa in the Epa and Ce6/Epa NP groups, the cadherin junction was tighter. Therefore, the invasiveness was much weaker compared with that for groups without Epa. These results confirmed the strong ability of Epa in the Ce6/Epa NPs to block EMT in order to decrease the invasiveness of the MDA-MB-231 cells.

We wished to demonstrate the combined effects of the Ce6/Epa NPs *in vivo* in BLBC tumor-bearing SCID mice. Three groups (NS, the Ce6/Epa NPs, and the Ce6/Epa NPs + NIR) were established. PDT effects was evaluated by comparing the Ce6/Epa NPs + NIR group with the Ce6/Epa NPs group. EMT blockade was investigated by comparing the Ce6/Epa NPs group with the NS group because Ce6 in the Ce6/Epa NPs could not work without NIR irradiation. First, the biodistribution of the Ce6/Epa NPs was investigated with an *in vivo* imaging system. As shown in Fig. 3a, the Ce6/Epa NPs were found to be

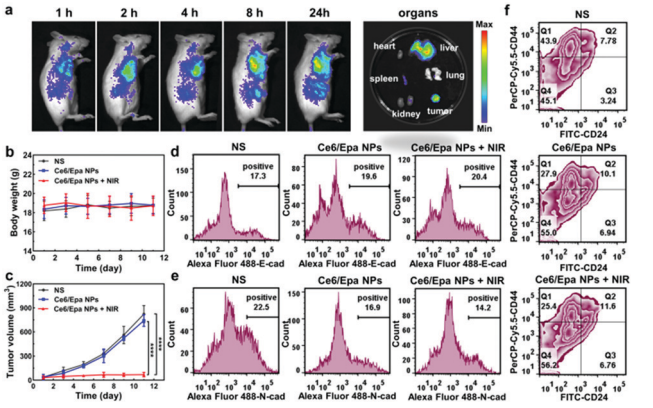

Fig. 3 (a) Biodistribution of the Ce6/Epa NPs. (b) Bodyweight (n = 5) and (c) tumor volume of each group during treatment (n = 5). (d) E-cad expression and (e) N-cad expression in each group. (f) CSC population in each group.

distributed preferentially at tumor sites. At 24 h post-administration, organs were excised from the mice, and there was strong in tumor fluorescence, which indicated the excellent tumor-accumulation properties of the Ce6/Epa NPs. Based on the biodistribution results, we selected to irradiate the tumor sites 8 h after administration in anti-tumor experiments. When the tumor reached ~50 mm^3, mice in the NS group or the Ce6/Epa NP group were administered (i.v.) with NS or the Ce6/Epa NPs (3 mg kg^{-1} for Ce6 and 2.4 mg kg^{-1} for Epa), and the tumors in the Ce6/Epa NPs + NIR group were irradiated further (100 mW cm^{-2}, 5 min) 8 h after administration. An obvious bodyweight change in the three groups was not observed (Fig. 3b), which showed the low cytotoxicity and good biocompatibility of the Ce6/Epa NPs. Tumors grew rapidly in the NS group (Fig. 3c) and, due to the low cytotoxicity of Ce6 and Epa, the tumor volume in the Ce6/Epa NP group was not significantly different from that in the NS group. However, Ce6/Epa NPs + NIR hampered tumor growth compared with the Ce6/Epa NP group, suggesting its excellent PDT-based efficacy in killing tumors. Moreover, to evaluate the EMT blockade of Epa in the Ce6/Epa NPs, expression of E-cad and N-cad on tumor cells from different groups was measured by flow cytometry after the final treatment (Fig. 3d and e, respectively). Expression of the epithelial marker E-cad was upregulated slightly in the Ce6/Epa NP-treated mice compared with that in the NS group. Expression of the mesenchymal marker N-cad was downregulated markedly, indicating that EMT was blocked in the Ce6/Epa NP-involved groups. Besides contributing to metastasis, EMT can endow tumor cells with stem cell-like properties.[20] Therefore, a breast cancer stem cell (CSC) phenotype ($CD44^{high}$/$CD24^{low}$)[21] was examined using flow cytometry. The Q1 population ($CD44^{high}$/$CD24^{low}$) in Fig. 3f represents CSC. The $CD44^{high}$/$CD24^{low}$ population decreased significantly in the Ce6/Epa NP-involved group, further indicating blockade of EMT.

Based on the advantages of PDT-based tumor killing and Epa-mediated EMT blockade by the Ce6/Epa NPs, lung metastasis in the three groups was observed further. More than

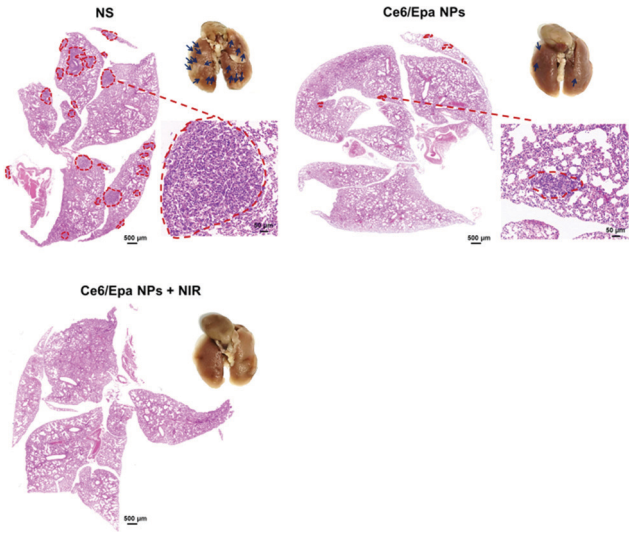

Fig. 4 Photographs of lungs and H&E staining of lung sections from differently treated mice. Blue arrows denote metastatic tumor nodules. Red dotted lined denote foreign tumor tissues.

17 metastatic tumor nodules were observed in the lungs of NS mice (Fig. 4). Thanks to EMT blockade, metastatic nodules in the lung from the Ce6/Epa NP group was reduced to <5. This finding demonstrated the effectiveness of the EMT-blockade strategy in preventing BLBC metastasis. Strikingly, no nodule was observed in the Ce6/Epa NPs + NIR group because of the combined effects of PDT-based tumor killing and Epa-based EMT blockade. In the stained (hematoxylin and eosin) lungs shown in Fig. 4, a red dotted line denotes foreign tumor tissues in lungs. The area of foreign tumor tissue in the Ce6/Epa NP group was much less than that in the NS group, and no foreign tissue was observed in the Ce6/Epa + NIR group. Taken together, these results demonstrated the feasibility of a combined strategy of PDT-based tumor killing and EMT-based blockade in prevention of metastasis from BLBC.

In summary, a two-pronged concept combining PDT and EMT blockade for prevention of metastasis from BLBC was proposed. We fabricated a minimalist drug, Ce6/Epa NPs, with 100% drug loading *via* co-assembly nanotechnology. Due to enhanced tumor accumulation and cellular internalization of the nanoscale Ce6/Epa NPs, highly efficient Ce6 delivery was achieved, and PDT-based tumor killing has increased. EMT, which endows BLBC with invasiveness, was blocked with Epa in the Ce6/Epa NPs to prevent metastasis initiation. This two-pronged nanoplatform helped to prevent BLBC metastasis *in vitro* and *in vivo*, and could provide a novel and valuable solution for BLBC metastasis.

This work was financially supported by the National Natural Science Foundation of China (NSFC, No. 82061148009 and No. 21872083). We acknowledge the Pharmaceutical Biology Sharing Platform and the Advanced Medical Research Institute of Shandong University.

Conflicts of interest

There are no conflicts to declare.

Notes and references

1 B. Kreike, M. van Kouwenhove, H. Horlings, B. Weigelt, H. Peterse, H. Bartelink and M. J. van de Vijver, *Breast Cancer Res.*, 2007, **9**, R65.
2 P. Kumar and R. Aggarwal, *Arch. Gynecol. Obstet.*, 2016, **293**, 247–269.
3 S. Hurvitz and M. Mead, *Curr. Opin. Gynecol. Obstet.*, 2016, **28**, 59–69.
4 F. Bray, J. Ferlay, I. Soerjomataram, R. L. Siegel, L. A. Torre and A. Jemal, *Ca-Cancer J. Clin.*, 2018, **68**, 394–424.
5 H. P. Sun, J. H. Su, Q. S. Meng, Q. Yin, L. L. Chen, W. W. Gu, P. C. Zhang, Z. W. Zhang, H. J. Yu, S. L. Wang and Y. P. Li, *Adv. Mater.*, 2016, **28**, 9581–9588.
6 S. H. Wang, J. D. Shao, Z. B. Li, Q. Z. Ren, X. F. Yu and S. J. Liu, *Nano Lett.*, 2019, **19**, 5587–5594.
7 N. Sethi and Y. B. Kang, *Nat. Rev. Cancer*, 2011, **11**, 735–748.
8 B. L. Eckhardt, P. A. Francis, B. S. Parker and R. L. Anderson, *Nat. Rev. Drug Discovery*, 2012, **11**, 479–497.
9 S. A. Eccles and D. R. Welch, *Lancet*, 2007, **369**, 1742–1757.
10 J. Liu, H. J. Li, Y. L. Luo, C. F. Xu, X. J. Du, J. Z. Du and J. Wang, *ACS Nano*, 2019, **13**, 8648–8658.
11 Y. Long, Z. Z. Lu, S. S. Xu, M. Li, X. H. Wang, Z. R. Zhang and Q. He, *Nano Lett.*, 2020, **20**, 2219–2229.
12 T. Z. Jiang, L. Chen, Y. K. Huang, J. H. Wang, M. J. Xu, S. L. Zhou, X. Gu, Y. Chen, K. F. Liang, Y. Y. Pei, Q. X. Song, S. S. Liu, F. F. Ma, H. P. Lu, X. L. Gao and J. Chen, *Nano Lett.*, 2019, **19**, 3548–3562.
13 W. T. Sun, K. Ge, Y. Jin, Y. Han, H. S. Zhang, G. Q. Zhou, X. J. Yang, D. D. Liu, H. F. Liu, X. J. Liang and J. C. Zhang, *ACS Nano*, 2019, **13**, 7556–7567.
14 J. H. Tsai and J. Yang, *Genes Dev.*, 2013, **27**, 2192–2206.
15 X. B. Wu, X. L. Li, Q. Fu, Q. H. Cao, X. Y. Chen, M. J. Wang, J. Yu, J. P. Long, J. Yao, H. X. Liu, D. P. Wang, R. C. Liao and C. F. Dong, *J. Exp. Med.*, 2017, **214**, 1065–1079.
16 Z. W. Zhou, H. Wu, R. X. Yang, A. Xu, Q. Y. Zhang, J. W. Dong, C. G. Qian and M. J. Sun, *Sci. Adv.*, 2020, **6**, eabc4373.
17 Q. Li, D. Zhang, J. Zhang, Y. Jiang, A. X. Song, Z. H. Li and Y. X. Luan, *Nano Lett.*, 2019, **19**, 6647–6657.
18 R. Y. Zhang, R. R. Xing, T. F. Jiao, K. Ma, C. J. Chen, G. H. Ma and X. H. Yan, *ACS Appl. Mater. Interfaces*, 2016, **8**, 13262–13269.
19 V. T. Banala, S. Urandur, S. Sharma, M. Sharma, R. P. Shukla, D. Marwaha, S. Gautam, M. Dwivedi and P. R. Mishra, *Biomater. Sci.*, 2019, **7**, 2889–2906.
20 K. Polyak and R. A. Weinberg, *Nat. Rev. Cancer*, 2009, **9**, 265–273.
21 C. Fillmore and C. Kuperwasser, *Breast Cancer Res.*, 2007, **9**, 303.

